RADC-TR-90-12
In-House Report
March 1990

OPTICAL LINKS FOR MICROWAVE APPLICATION

Edward N. Toughlian, 1/Lt, USAF; Steven T. Johns; Mark C. Schmitt

APPROVED FOR PUBLIC RELEASE; DISTRIBUTION UNLIMITED.

Rome Air Development Center
Air Force Systems Command
Griffiss Air Force Base, NY 13441-5700

UNCLASSIFIED
SECURITY CLASSIFICATION OF THIS PAGE

REPORT DOCUMENTATION PAGE

Form Approved OMB No. 0704-0188

1a. REPORT SECURITY CLASSIFICATION: UNCLASSIFIED	1b. RESTRICTIVE MARKINGS: N/A
2a. SECURITY CLASSIFICATION AUTHORITY: N/A	3. DISTRIBUTION/AVAILABILITY OF REPORT: Approved for public release; distribution unlimited.
2b. DECLASSIFICATION/DOWNGRADING SCHEDULE: N/A	
4. PERFORMING ORGANIZATION REPORT NUMBER(S): RADC-TR-90-12	5. MONITORING ORGANIZATION REPORT NUMBER(S): N/A
6a. NAME OF PERFORMING ORGANIZATION: Rome Air Development Center; 6b. OFFICE SYMBOL (If applicable): OPA	7a. NAME OF MONITORING ORGANIZATION: Rome Air Development Center (OPA)
6c. ADDRESS (City, State, and ZIP Code): Griffiss AFB NY 13441-5700	7b. ADDRESS (City, State, and ZIP Code): Griffiss AFB NY 13441-5700
8a. NAME OF FUNDING/SPONSORING ORGANIZATION: Rome Air Development Center; 8b. OFFICE SYMBOL (If applicable): OPA	9. PROCUREMENT INSTRUMENT IDENTIFICATION NUMBER: N/A
8c. ADDRESS (City, State, and ZIP Code): Griffiss AFB NY 13441-5700	10. SOURCE OF FUNDING NUMBERS: PROGRAM ELEMENT NO. 62702F; PROJECT NO. 4600; TASK NO. P2; WORK UNIT ACCESSION NO. 02

11. TITLE (Include Security Classification): OPTICAL LINKS FOR MICROWAVE APPLICATION

12. PERSONAL AUTHOR(S): Edward N. Toughlian, 1/Lt, USAF; Steven T. Johns; Mark C. Schmitt

13a. TYPE OF REPORT	13b. TIME COVERED	14. DATE OF REPORT (Year, Month, Day)	15. PAGE COUNT
In-House	FROM Mar 89 TO Jan 90	March 1990	36

16. SUPPLEMENTARY NOTATION: N/A

17. COSATI CODES			18. SUBJECT TERMS (Continue on reverse if necessary and identify by block number)
FIELD	GROUP	SUB-GROUP	Optical Links Optical Microwave Links
20	06		

19. ABSTRACT (Continue on reverse if necessary and identify by block number)

The RADC Directorate of Communications, Communications ECCM Section, in cooperation with the RADC Photonics Laboratory, Lightwave Signal Processing Group, is in the process of replacing the existing RF cabling system of their anechoic chamber with optical links. Fiber optic links will be employed in an effort to upgrade the DCCD anechoic chamber test facility. It is expected that any electromagnetic interference (EMI) emanating from the existing microwave system can be reduced measurably by replacing the antenna coaxial cabling and its associated components with optical link systems. This effort should not only improve the DCCD test bed, but will yield valuable data about the future of optical component applications in the microwave domain. This report will detail the Photonics Laboratory's portion of this effort.

While this report is related to this specific application, a more detailed characterization and analysis of the optical links will be carried out to provide information as to feasibility of using optical links as fiber feeds in microwave systems. We will report on the performance of these (Cont'd)

20. DISTRIBUTION/AVAILABILITY OF ABSTRACT: ☐ UNCLASSIFIED/UNLIMITED ☒ SAME AS RPT. ☐ DTIC USERS	21. ABSTRACT SECURITY CLASSIFICATION: UNCLASSIFIED
22a. NAME OF RESPONSIBLE INDIVIDUAL: EDWARD N. TOUGHLIAN, 1/Lt, USAF	22b. TELEPHONE (Include Area Code): (315) 330-4365; 22c. OFFICE SYMBOL: RADC(OPA)

DD Form 1473, JUN 86 — Previous editions are obsolete. — SECURITY CLASSIFICATION OF THIS PAGE: UNCLASSIFIED

19. (Cont'd). fiber optic components in the area of their noise contribution, bandwidth, and dynamic range capabilities as related to the needs of a typical communications system.

1. Introduction

It is expected that the performance of communication and antenna remoting systems can be greatly enhanced by exploiting the properties of fiber optic components. Lower noise, greater immunity to electromagnetic interference, and lower weight systems are some of the advantages that can be realized. Optical systems also have the capacity to handle much larger bandwidths as well as offer a much lower signal attenuation.

Fiber optic links will be employed in an effort to upgrade the DCCD anechoic chamber test facility. It is expected that any electro-magnetic interference (EMI) emanating from the existing microwave system can be reduced measurably by replacing the antenna coaxial cabling and its associated components with optical link systems. This effort should not only improve the DCCD test bed, but will yield valuable data about the future of optical component applications in the microwave domain.

Prior to installation in the anechoic chamber, it was necessary to evaluate the optical link systems to ensure they meet the interface requirements of the existing system. This includes dynamic range and noise limitations of the receive only Flexible Adaptive Spatial Signal Processor (FASSP). Other tests were performed to evaluate the limits of optical links for future systems uses.

The anechoic chamber's antenna consists of twelve phased array elements. Four of these elements will be replaced by optical link systems. This will allow for direct comparison between operation of the existing system and optical links once installation is accomplished. The results of the testing, evaluation, and alignment of the optical links prior to their installation in the anechoic chamber is detailed in this report. We will compare the measured characteristics of these fiber optic links to the performance of the RF cabling as well as the requirements of a typical communications system.

2. System Description

Component selection was based on anechoic chamber and associated equipment interface requirements. Since the antenna system was designed to run at 8.14 GHz, the task of optical link selection was significantly simplified. The Ortel TSL-1000 optical transmitter and the Ortel RSL-25 optical receiver were selected based on their frequency range of 10 KHz to 10 GHz.

The maximum received signal likely to be seen at the output of each antenna element (feedhorn) is less than -40 dBm. Therefore, 50 dB gain, narrow band (centered at 8 GHZ), Miteq amplifiers were selected to boost the signal. This will supply the Ortel transmitters with power near

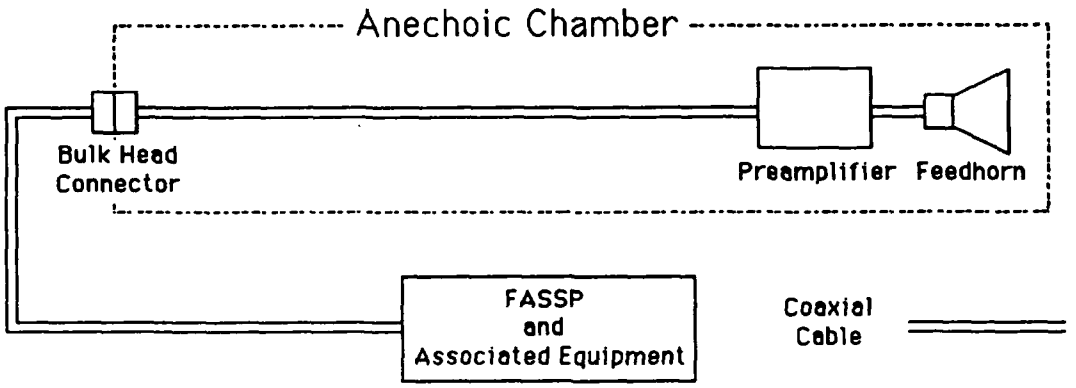

Figure 1a: Block diagram of one element of the phased array antenna prior to modification.

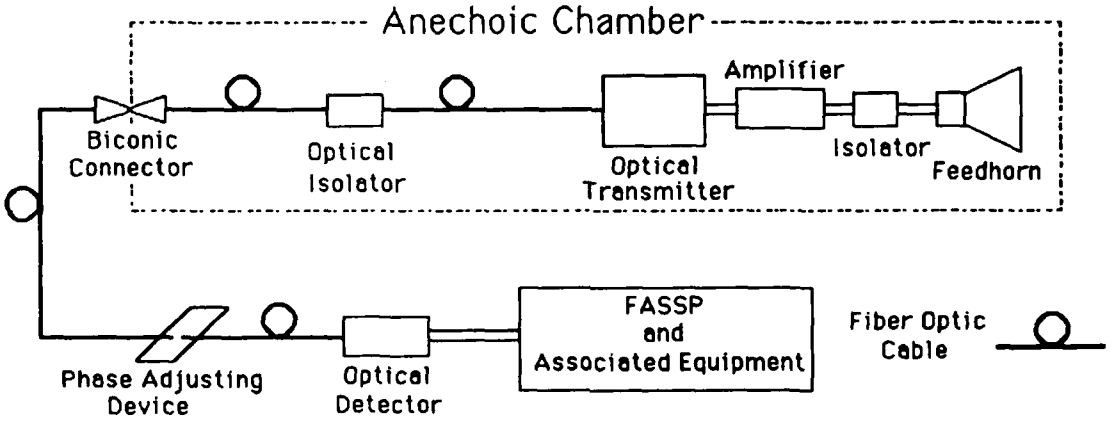

Figure 1b: Block diagram of one element of the optically fed phased array antenna.

their maximum RF input level of 12 dBm and thereby allow us to maximize the usable dynamic range of the links.

Other devices will be incorporated in each elemental leg of the antenna system (see Figure 1). These include electrical and optical isolators to prevent impedance mismatch reflections from the feedhorn, and optical reflections to the laser, respectively. 50 meter lengths of fiber and phase adjusting mechanisms to time match the links are also an integral part of the system.

3. Measurements

The three basic types of measurements that were performed are third order intermodulation products, dynamic range and noise figure. These measurements were accomplished on each complete link and on all sub-components of those links. This thorough characterization of all components will provide a record of their performance for future system maintenance, modifications, and upgrades.

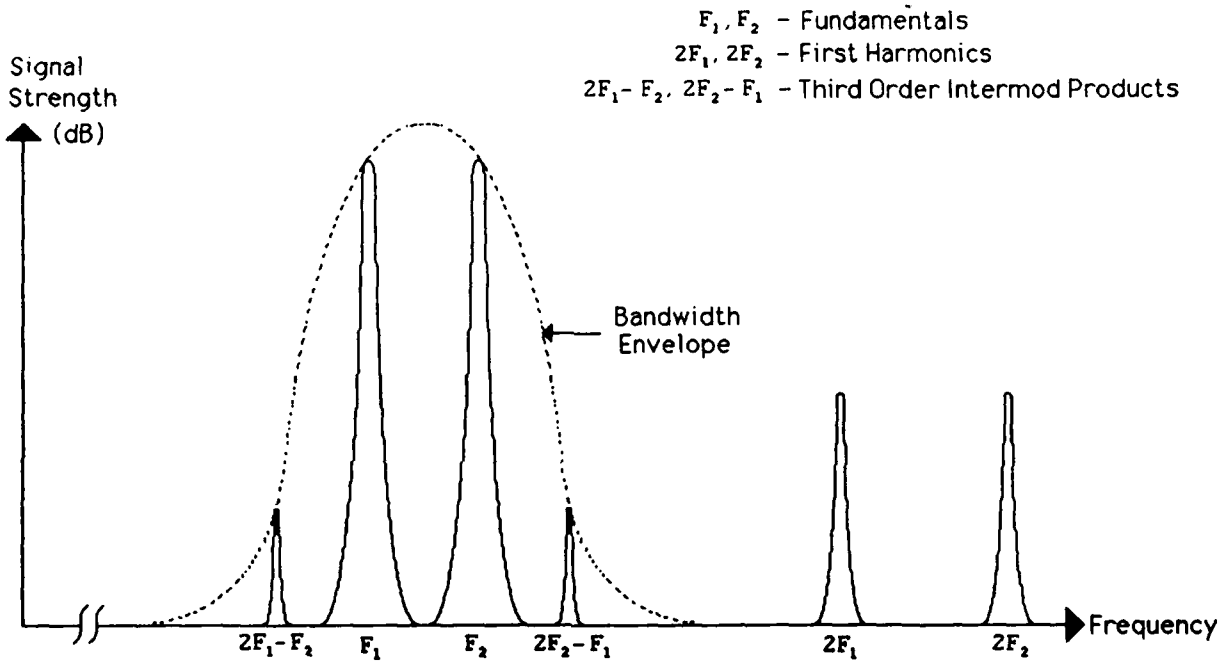

Figure 2: Frequency Spectrum representation of third order intermodulation products.

3.1 Third Order Intermodulation Products

When signals of different frequencies are mixed in a non-linear device intermodulation products are generated. The third order intermodulation terms are caused by the mixing of the first harmonic of one frequency and the fundamental of the other. If the two fundamental frequencies are close enough together these intermod products can appear within the bandwidth of the system and cause distortion (see Figure 2).

A standard approach to characterize the third order intermodulation products is by quantifying the third order intercept point. This point is the input power located at the intercept of the extended fundamental frequency response characteristic curve and the third order intermod product response characteristic curve (see Figure 3). The product of the two fundamentals of the

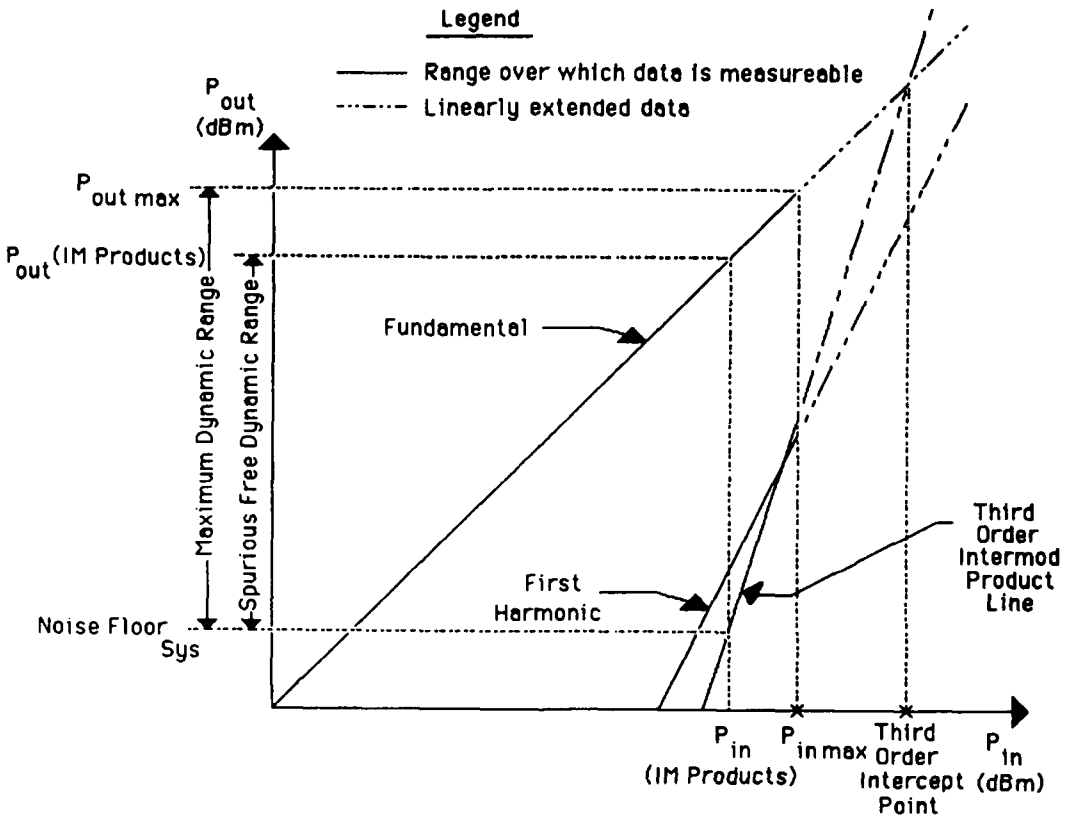

Figure 3: Characteristic curves for the fundamental, first harmonic, and third order intermod products.

same amplitude yields a first harmonic characteristic curve with a slope of two on a log scale (since the exponent of a number can be pulled outside the log term). Similarly, the product of the first harmonics with one of the fundamentals yields a characteristic curve with a slope of three on a log plot. Therefore, since the slopes of the two curves are known, the third order intercept point can be found mathematically by knowing just one point on each curve[1]. A more reliable and revealing approach is to measure numerous points on each curve and then find the intercept point using a best fit line for each curve. This was the approach we chose to make our measurements.

To make these measurements two signal generators and a microwave coupler are used to

provide the two fundamental frequencies. Since the largest possible bandwidth of the FASSP is 50 MHz centered at 8.14 GHz, the fundamentals F_1 and F_2 were chosen to be 8.115 and 8.165 GHz respectively. To prevent intermod products from being created in the generators, two isolators were placed on each signal generator output (see Figure 4). To further prevent any first

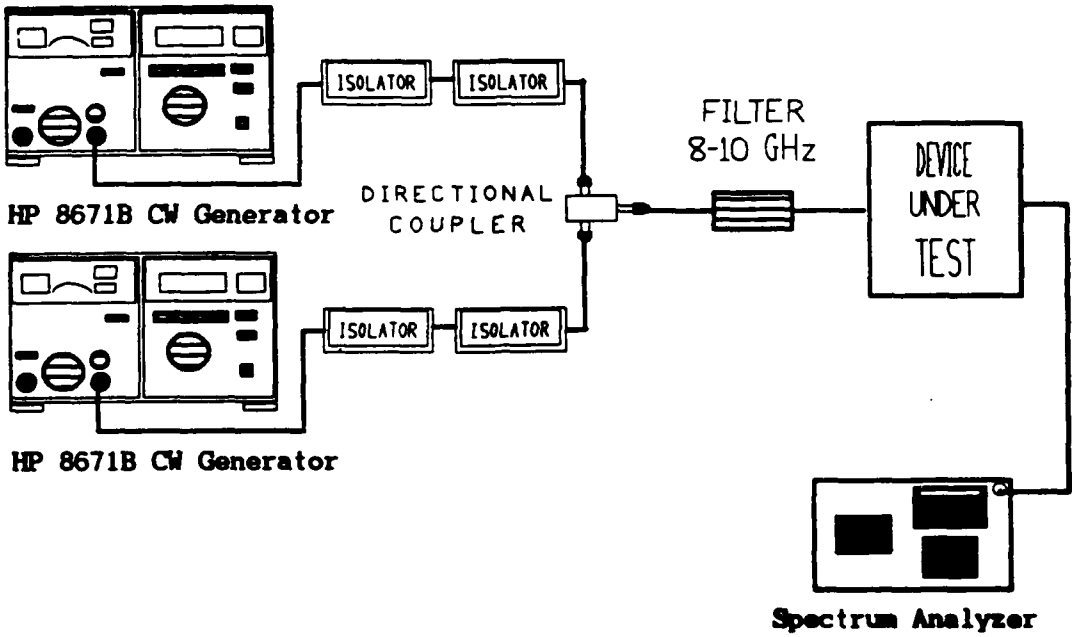

Figure 4: Block diagram of third order intermodulation and dynamic range measurement configuration.

harmonic signals from being sent from the signal generators to the Device Under Test (DUT), a 2 GHz bandpass filter centered at 9 GHz is included after the coupler.

The power out of each generator was set equal to the maximum allowable input power for the DUT plus 8 dB (11 dB to account for measured losses between the signal generator and the DUT; minus 3 dB because both fundamentals are applied simultaneously). The power out of each generator was then lowered in increments that would yield a sufficient number of points to deliver an accurate picture of the power curves. The power in the two fundamentals, first harmonics, and third order products was measured at each point using a spectrum analyzer.

3.2 Dynamic Range

There are assorted definitions of dynamic range[2], the most common of which is the ratio of maximum device/system power out (typically defined to be the power out prior to the power curve

deviating from linear by a specified magnitude) to the system noise floor (see Figure 3):

(1) $$\text{Dynamic Range}_{max} = P_{out\ max} / \text{Noise Floor}_{sys}$$

or

(2) $$\text{Dynamic Range}_{max}(dB) = P_{out\ max}(dBm) - \text{Noise Floor}_{sys}(dBm)$$

The system noise floor is the power at which the signal of interest is no longer detectable above the system noise (this is sometimes referred to as system sensitivity). It can be quantified by the equation :

(3) $$\text{Noise Floor}_{sys}(dBm) = 10\ \text{Log}(kTB) + F_{DUT}(dB)$$

where k = Boltzmann's constant ($1.38 * 10^{-23}$ Joule/K)
T = temperature (K)
B = system bandwidth (Hz)
F_{DUT} = noise figure of the DUT (see section 3.3)

Therefore; equation (2) can be rewritten as :

(4) $$\text{Dynamic Range}_{max}(dB) = P_{out\ max}(dBm) - [10\ \text{Log}(kTB) + F_{DUT}(dB)]$$

This equation is readily applied if the noise figure for the DUT is known. Often times that is not the case, and in these instances the system noise level (Johnson Noise plus Noise Figure) can be read directly from the spectrum analyzer, typically with very good accuracy[3]. This value can be calculated or accomplished with the noise marker function (if the DUT noise level is at least 10 dB above the spectrum analyzer noise[4]) found on most high performance spectrum analyzers. This function corrects for log amp and detector errors as well as normalizing the noise to a 1 Hz bandwidth; in effect removing the noise attributed by the spectrum analyzer. This is the approach we'll use for our link measurements.

Another definition of dynamic range that is of greater consequence when dealing with communication systems is the spurious free dynamic range (SFDR). This form of dynamic range is found from third order intermodulation product measurements. The SFDR is the ratio of the fundamental power out that occurs at the input signal where intermodulation products are just detected for a given system noise floor, to the level of the noise floor (see Figure 3):

(5) SFDR = P_{out}(IM Products)/ Noise $Floor_{Sys}$

or

(6) SFDR(dB) = P_{out} (IM Products)(dBm) - Noise $Floor_{Sys}$(dBm)

This measurement yields a value which is always less than or at best equal to the maximum dynamic range of the device (the two are equal when no intermodulation distortion occurs). The first term in the above equation can be found from the best fit characteristic curves for the fundamental and third order products; respectively as:

(7) P_{out} (IM Products)(dBm) = m_1*P_{in} (IM Products)(dBm) + b_1

and

(8) $P_{out\ (Third\ Order\ Curve)}$(dBm) = m_3*P_{in} (dBm) + b_3

where eq (7) is the point on the fundamental characteristic curve corresponding to the onset of third order products for a given noise floor,
eq (8) is the characteristic equation for the third order intermod product line,
m represents the slope of the lines, and
b represents the point at which the line would intercept the P_{out} axis for P_{in} equal to 0 dBm.

If we plug into equation (8) the point associated with the noise floor of the system:

(9) Noise $Floor_{Sys}$(dBm) = m_3*P_{in}(IM Products)(dBm) + b_3

Solving for P_{in}(IM Products) and substituting into equation (7) gives:

(10) P_{out} (IM Products)(dBm) = m_1[(Noise $Floor_{Sys}$ - b_3)/m_3] + b_1

The equation for spurious free dynamic range is now found from equations (3), (6), and (10):

(11) SFDR(dB) = [F + 10 Log kTB][(m_1/m_3)-1] - b_3m_1/m_3 + b_1

The two types of dynamic range for each DUT are reported at both a 10 MHz and 50 MHz

signal bandwidth.

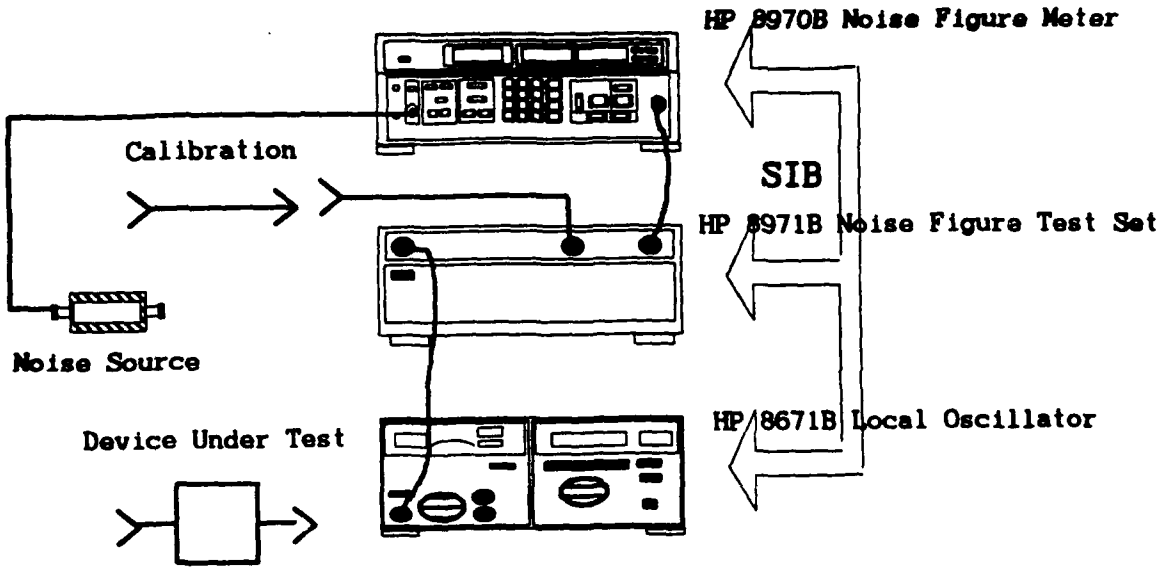

Figure 5: Noise Figure measurement configuration.

3.3 Noise Figure

Noise figure (F) is defined to be the ratio of noise out of a device/system divided by it's gain, to the ideal device/system noise for a given temperature, T_0 of 290 K and signal bandwidth (B):

$$F = N_{out} / kT_OBG$$

or

$$F(dB) = N_{out}(dBm) - 10\ Log(kT_OBG)$$

where $G = S_o / S_i$ = Signal Out / Signal In

Noise figure provides a measure of the decrease or degradation in the signal to noise (S/N) ratio and can be used to relate system performance to component performance[5]. If N_{out} is proportional to B, as it is in many cases, then F will be independent of B. Noise figure provides information about the ability of a network to process weak signals.

Noise figure and gain measurements were accomplished using an HP 8970B noise figure meter, HP 8971B noise figure test set, HP 346B noise source, and HP 8671B synthesized CW generator (see Figure 5). The two usable bandwidths of the FASSP system are 10 MHz and 50 MHz. The noise figure and gain measurements were made using a signal bandwidth of 6 MHz. We have assumed that N_{out} is directly proportional to B and therefore use the same noise figure for all bandwidths.

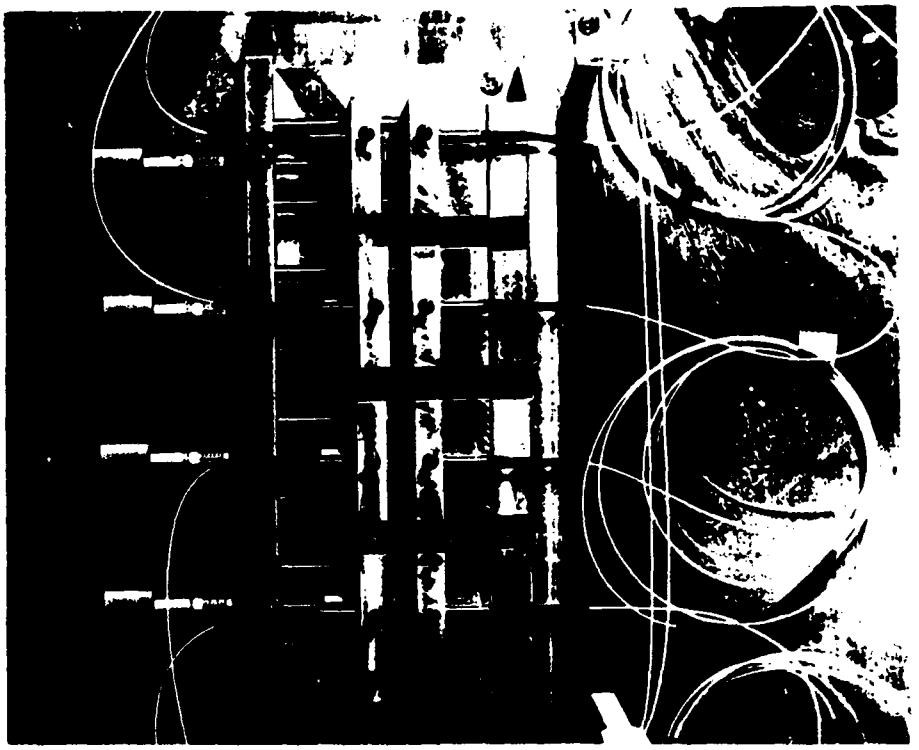

Figure 6: Optical phase matching device.

3.4 **Time Matching**

Mathematical models can predict antenna radiation patterns for a known system. For physical realization of a model system, it is necessary that feeds into the experimental system be time matched as closely as possible. Any significant deviation from a true time matched system will result in antenna pattern measurements that differ from predicted results. One degree at 8 GHz, given the specifications of the test bed, was chosen as a reasonable goal for the time matching of the antenna feeds.

The time matching has been realized using a device invented, designed, and manufactured in the Photonics Laboratory. The device (see Figure 6) provides for variable air gap spacing. The change in gap size effectively changes the electrical length of the system, hence the relative phase of the signal at the output of the detector. The two main features of the device are the micrometer screw adjust and the pig-tailed grin rod lens collimators. The micrometer screw provides 794 microns of translational movement for each turn of the knob. This equates to 7.62 degrees per turn at 8 GHz. The pig-tailed grin rod lenses collimate the beams to couple a maximum amount of light across the air gap and thereby increase the range of adjustment.

Time matching was accomplished using a Wiltron 360 network analyzer to compare phasing at the output of the four links.

4. Results

The results given in the following three sections: amplifiers, links, and time matched systems, describe peculiarities associated in the measurement procedures, calculations, and results associated with each specific DUT.

At the conclusion of the text in each section a table of the results for the four DUTs is included. This is followed by a page for each DUT showing an intermod graph and a noise figure plot.

4.1 Amplifiers

Data sheets provided with the amplifiers guarantee a minimum gain of 50 dB and linear operation (1 dB compression point) for output power less than +15 dBm. Therefore, maximum input to the amps was limited to -35 dBm. After accounting for the losses and double power term (see section 3.1); intermod measurements were performed starting with a maximum output from the signal generators of -27 dBm to yield an amplifier input of -38 dBm. Measurements were continued by lowering the output of both sources simultaneously in 5 dB increments. The values for the maximum dynamic range were found from the noise figure measurements and equation (4). The SFDR values were found from the coefficients of the best fit curves given below, and equation (11). P_{out} max is +15 dBm.

Based on measured data, the best fit equations for the amplifier fundamental and IM product lines are:

Amp SN	130260	$P_{out\ (Fundamental\ Curve)}(dBm) = 0.98 * P_{in}\ (dBm) + 50.23$
		$P_{out\ (Third\ Order\ Curve)}(dBm) = 3.13 * P_{in}\ (dBm) + 110.5$
	130261	$P_{out\ (Fundamental\ Curve)}(dBm) = 0.97 * P_{in}\ (dBm) + 50.54$
		$P_{out\ (Third\ Order\ Curve)}(dBm) = 3.08 * P_{in}\ (dBm) + 106.4$
	130262	$P_{out\ (Fundamental\ Curve)}(dBm) = 0.97 * P_{in}\ (dBm) + 47.35$
		$P_{out\ (Third\ Order\ Curve)}(dBm) = 3.02 * P_{in}\ (dBm) + 101.1$
	130263	$P_{out\ (Fundamental\ Curve)}(dBm) = 0.98 * P_{in}\ (dBm) + 48.63$
		$P_{out\ (Third\ Order\ Curve)}(dBm) = 3.16 * P_{in}\ (dBm) + 104.5$

In order to measure noise figure on the amplifiers, a 10 dB attenuator was placed between the amplifier and the noise figure meter. This pad kept the input to the noise figure meter below its maximum gain measurement capability of 50 dB. The plotted and tabulated gain values have been adjusted to reflect the actual gain of the devices (i.e., the 10 dB attenuator is not included). To insure the 10 dB pads would not affect the noise figure measurements, their noise figure was measured with no appreciable noise found.

Amps	Third Order Intercept Point (dBm)	Maximum Dynamic Range (dB)		Spurious Free Dynamic Range (dB)		Noise Figure (dB)	Gain (dB)
		10 MHz	50 MHz	10 MHz	50 MHz		
130260	-28	115	108	84	80	4.2	52
130261	-26	115	108	86	81	3.9	52
130262	-26	115	108	83	78	4.1	49
130263	-26	115	108	85	80	4.2	50
Average	-27	115	108	85	80	4	51

Table 1: Tabulated results for the four amplifiers.

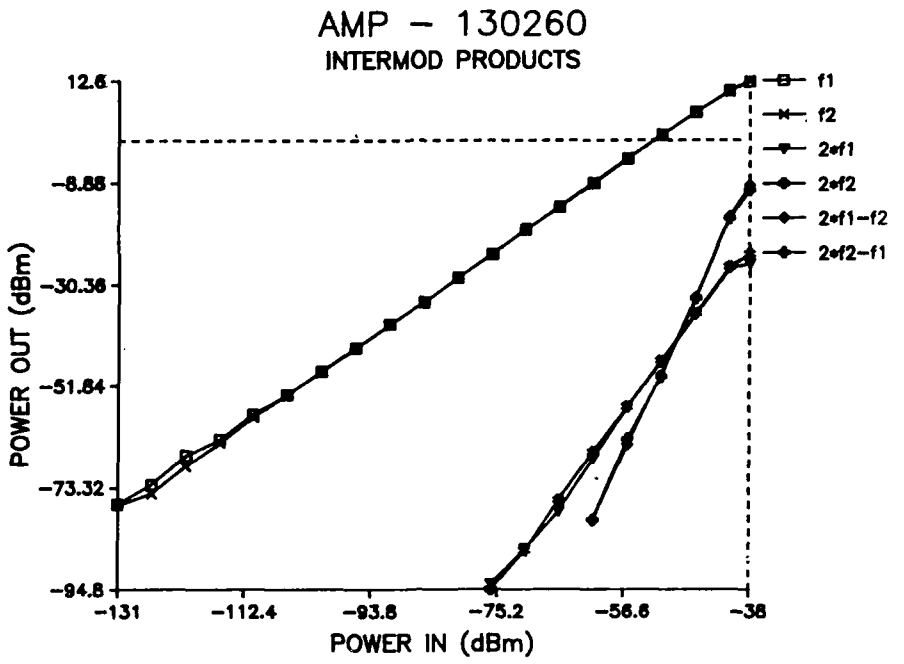

Figure 7: Intermod and Dynamic Range Characteristic Curves

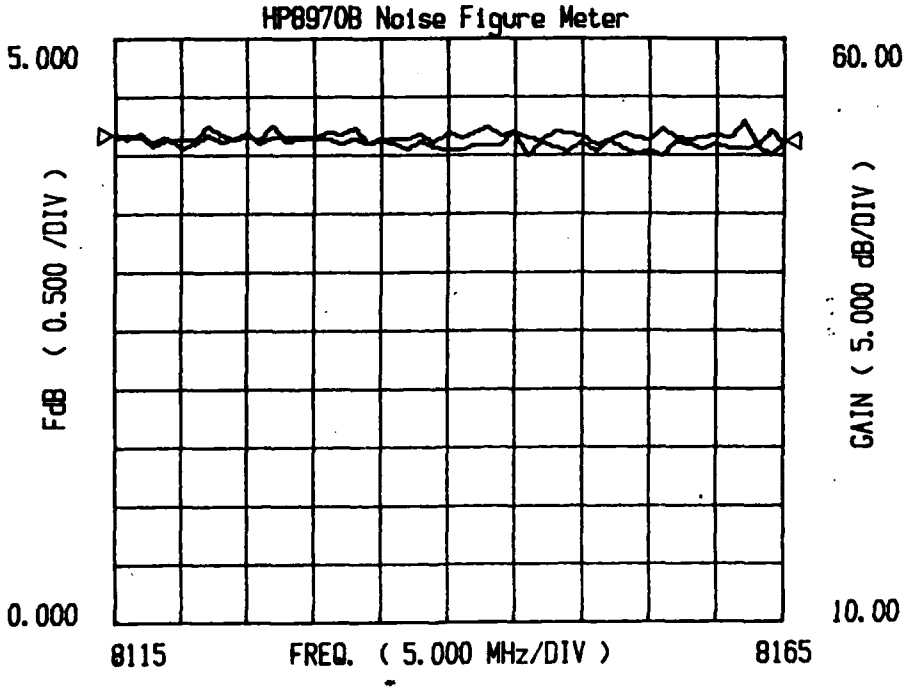

Figure 8: Noise Figure and Gain Plot

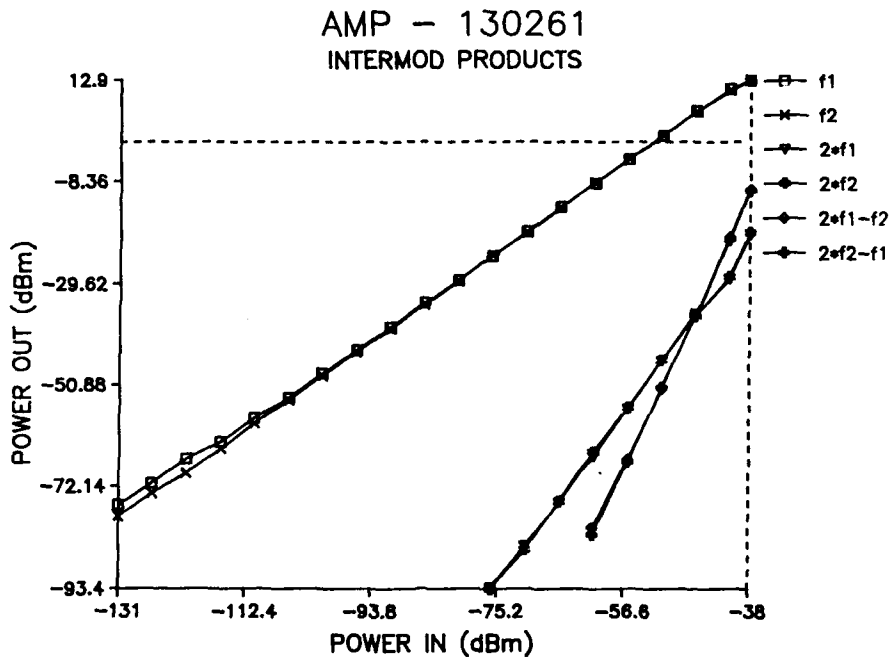

Figure 9: Intermod and Dynamic Range Characteristic Curves

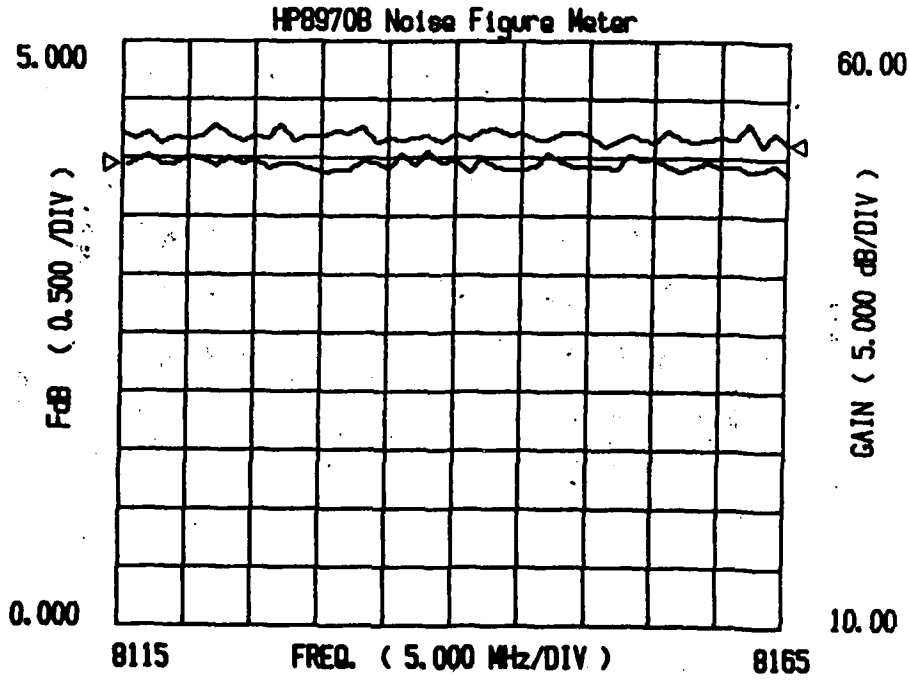

Figure 10: Noise Figure and Gain Plot

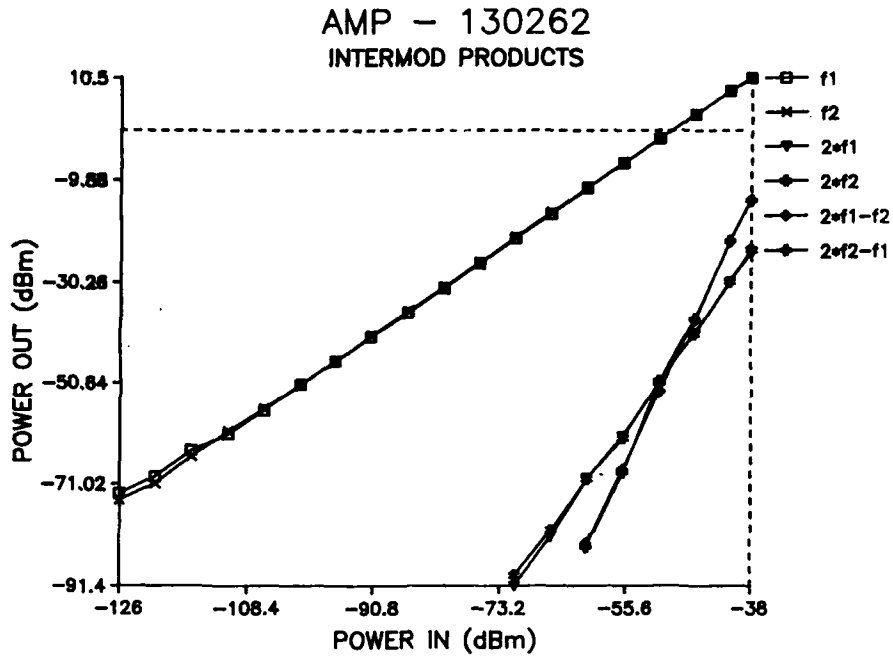

Figure 11: Intermod and Dynamic Range Characteristic Curves

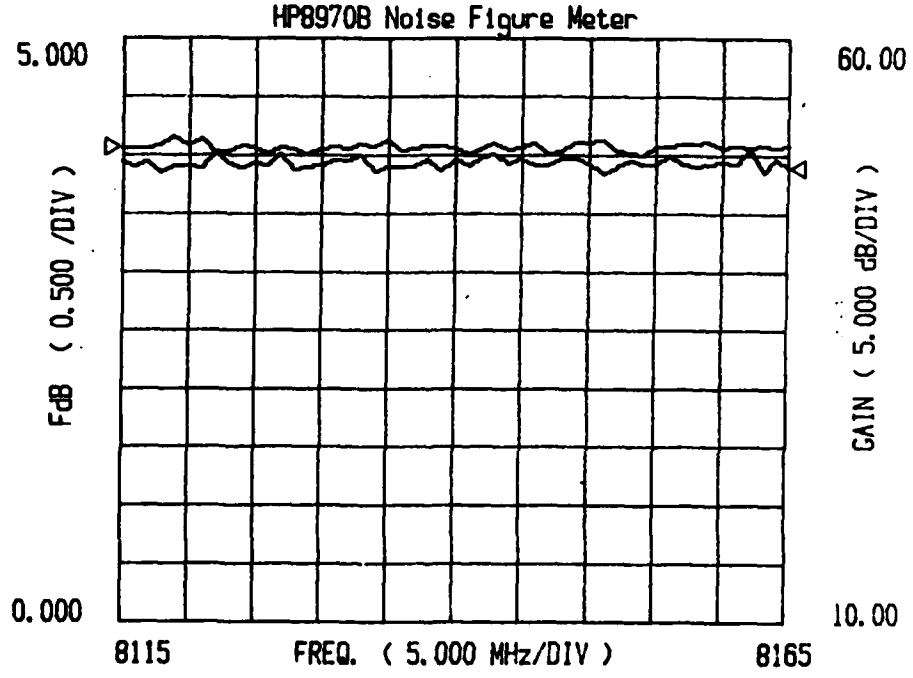

Figure 12: Noise Figure and Gain Plot

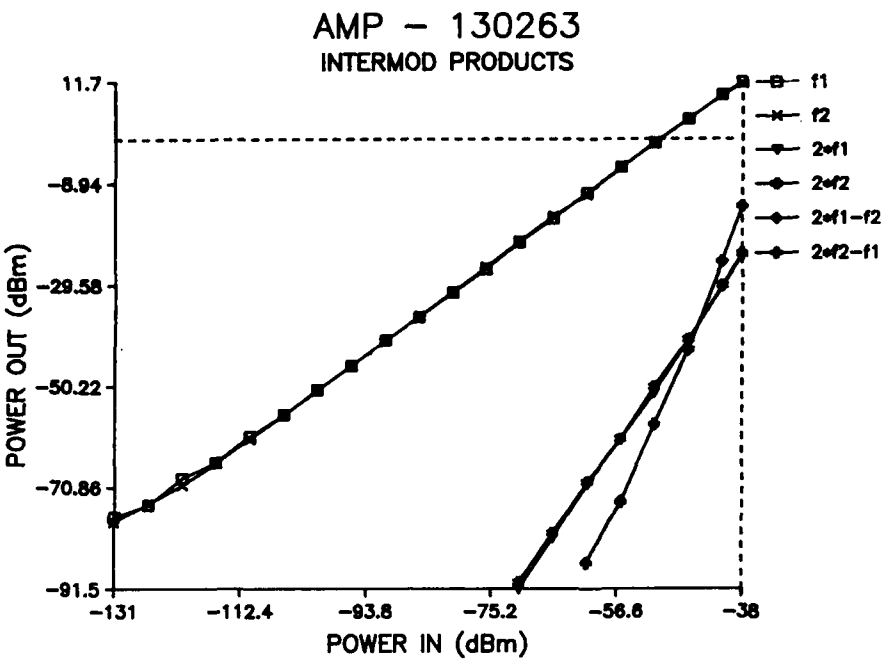

Figure 13: Intermod and Dynamic Range Characteristic Curves

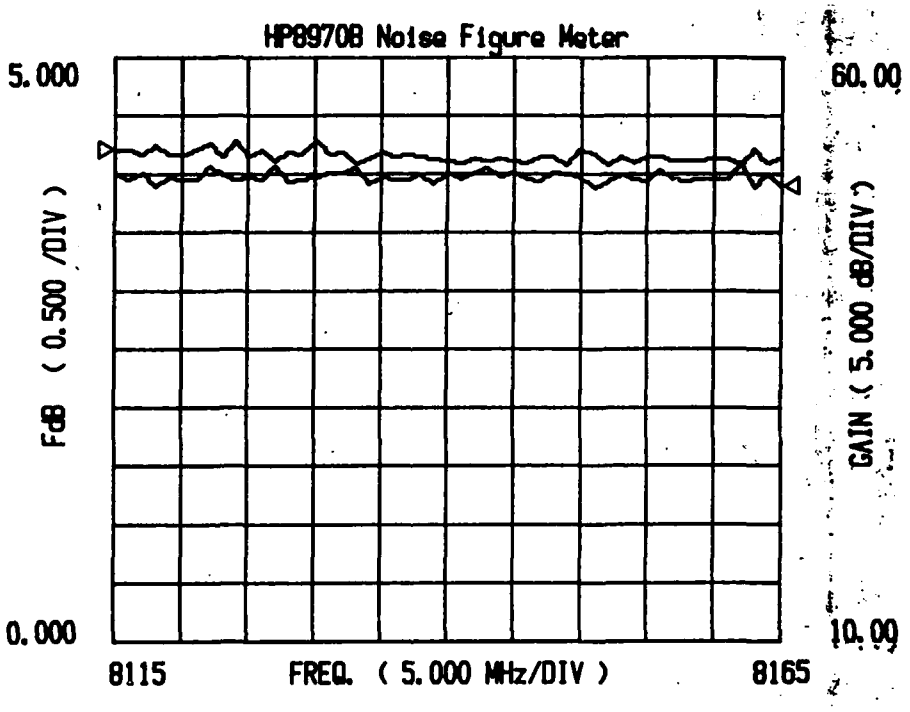

Figure 14: Noise Figure and Gain Plot

4.2 Links

From the Ortel transmitter data sheets, the maximum allowable input to the links is given to be +12 dBm. From section 3.1a, +20 dBm output from the signals generators is required to provide a +12 dBm input to the transmitter. The sources we used could provide a stable output no greater than +10 dBm. This limitation has no effect on the accuracy of the third order intercept points since they are interpolated values. For the maximum dynamic range we used the data sheet max input times the measured gain. The pigtailed fiber from the transmitters and detectors were fused together in order to measure the performance of the links.

The noise figure was not measured on the links due to the noise figure test set not being capable of measuring DUTs with a gain less than -30 dB. Since noise figure of the links was not measured, the gain values had to be found utilizing an alternate method. The gain can also be found from the "y intercept" of the fundamental characteristic curve. This can be shown as follows:

$$(12) \qquad P_{out}(dBm) = m_1 P_{in}(dBm) + b_1(dB)$$

where b_1 is the y intercept of the fundamental characteristic curve.

$$(13) \qquad P_{out}(dBm) = P_{in}(dBm) + b_1(dB)$$

since the slope (m) of the fundamental characteristic curve is approximately 1 for a linear device. Therefore:

$$(14) \qquad P_{out}(dBm) - P_{in}(dBm) = b_1(dB) = G_{DUT}(dB)$$

Since the noise figure of the links is unknown, the noise floor of the system can be found to be the normalized noise floor as measured by the spectrum analyzer (Noise $Floor_{SA}$ - see section 3.2) times the system bandwidth. The equations for dynamic range are found by appropriate modification of equations (4) and (11):

$$(15) \qquad \text{Dynamic Range}_{max}(dB) = [12(dBm) + G_{DUT}(dB)] - [\text{Normalized Noise Floor}_{SA}(dBm/Hz) + 10\,\text{Log}(B)]$$

$$(16) \qquad SFDR(dB) = [\text{Normalized Noise Floor}_{SA}(dBm/Hz) + 10\,\text{Log}(B)][(m_1/m_3)-1] -$$

$b_3 m_1 / m_3 + b_1$

The normalized noise floor values and best fit equations for the links are:

Transmitter/ Receiver SN		Normalized Noise Floor$_{SA}$
T-23/R-92	$P_{out\ (Fundamental\ Curve)}(dBm) = 1.00 * P_{in}\ (dBm) - 31.67$	-127 dBm/Hz
	$P_{out\ (Third\ Order\ Curve)}(dBm) = 2.90 * P_{in}(dBm) - 60.53$	
T-66/R-28	$P_{out\ (Fundamental\ Curve)}(dBm) = 0.99 * P_{in}(dBm) - 34.47$	-126 dBm/Hz
	$P_{out\ (Third\ Order\ Curve)}(dBm) = 2.80 * P_{in}(dBm) - 88.00$	
T-64/R-30	$P_{out\ (Fundamental\ Curve)}(dBm) = 0.99 * P_{in}(dBm) - 31.53$	-138 dBm/Hz
	$P_{out\ (Third\ Order\ Curve)}(dBm) = 2.60 * P_{in}(dBm) - 54.69$	
T-67/R-32	$P_{out\ (Fundamental\ Curve)}(dBm) = 0.99 * P_{in}(dBm) - 34.61$	-135 dBm/Hz
	$P_{out\ (Third\ Order\ Curve)}(dBm) = 2.92 * P_{in}(dBm) - 61.08$	

Links	Third Order Intercept Point (dBm)	Maximum Dynamic Range (dB)		Spurious Free Dynamic Range (dB)		Noise Figure (dB)	Gain (dB)
		10 MHz	50 MHz	10 MHz	50 MHz		
T-23;R-92	+15	37	30	27	22	*	-32
T-66;R-28	+30	34	27	33	28	*	-34
T-64;R-30	+14	48	41	31	27	*	-32
T-67;R-32	+14	42	35	29	24	*	-35
Average	+18	40	33	30	25	*	-33

Table 2: Tabulated results for the four links.

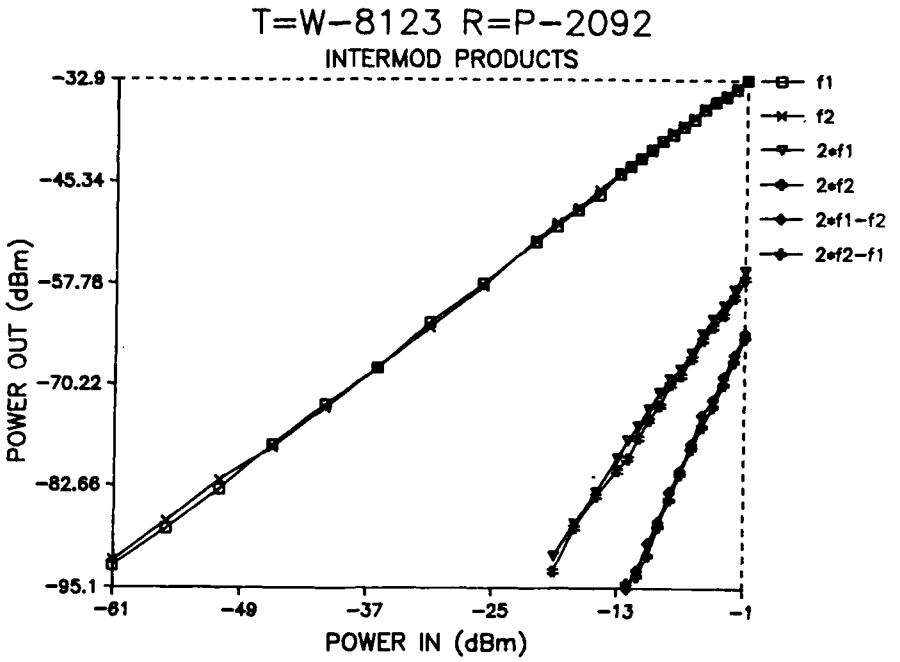

Figure 15: Intermod and Dynamic Range Characteristic Curve

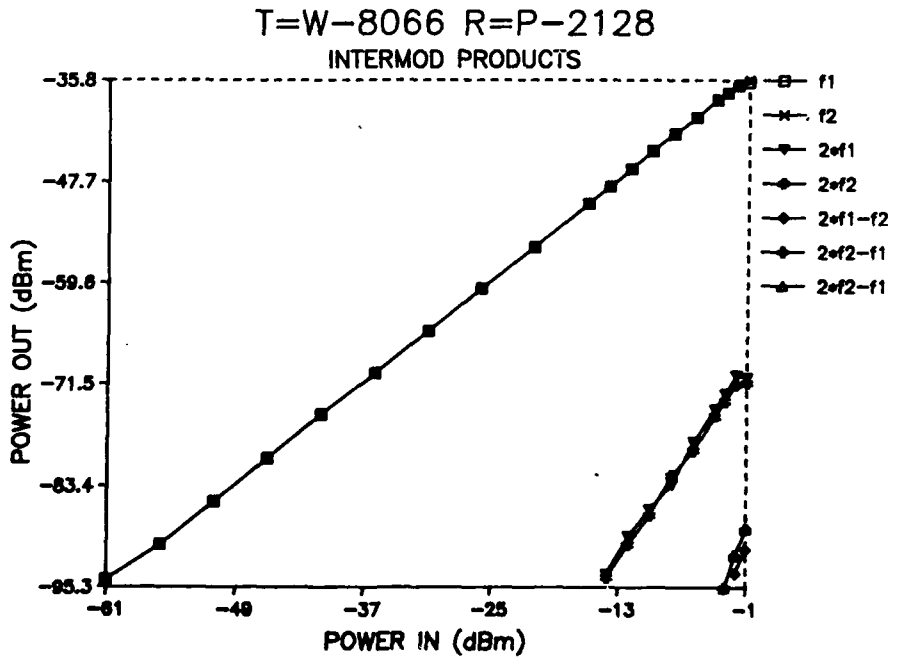

Figure 16: Intermod and Dynamic Range Characteristic Curves

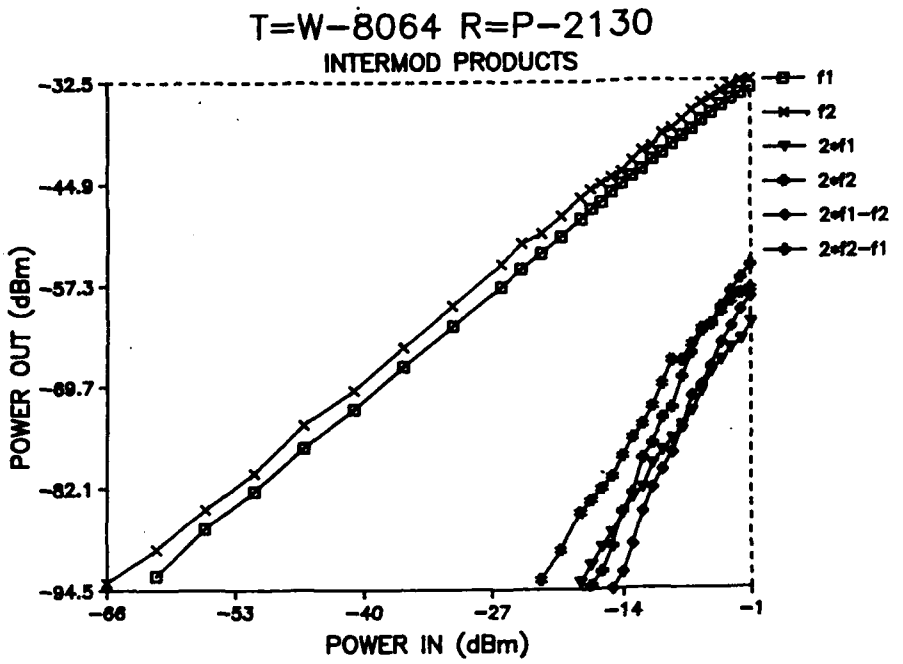

Figure 17: Intermod and Dynamic Range Characteristic Curves

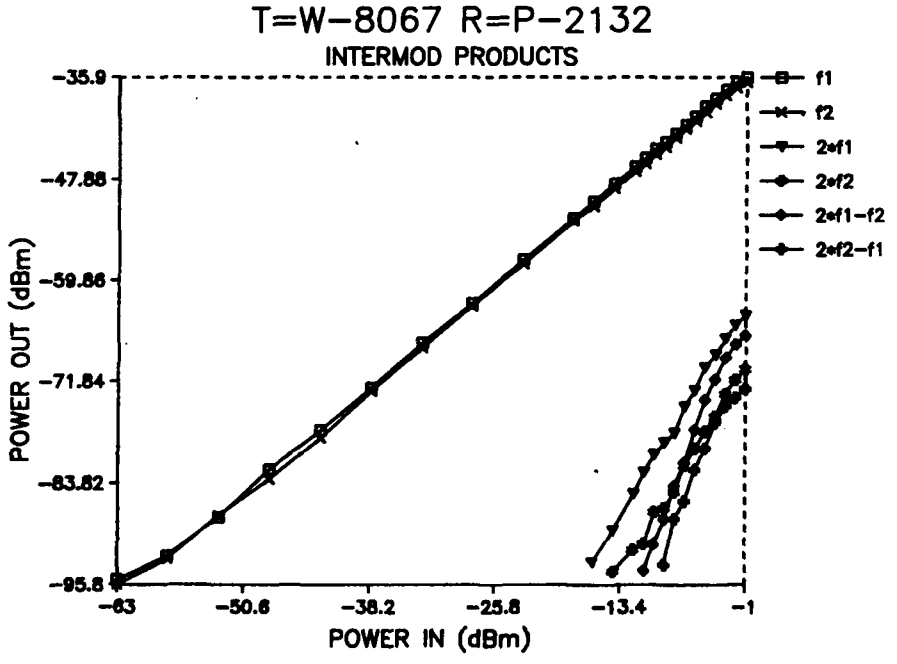

Figure 18: Intermod and Dynamic Range Characteristic Curves

4.3 Time Matched Systems

Input to the systems is limited to -38 dBm (+12 dBm maximum to the links minus the 50 dB amplifier gain). Accounting for the loss and double power term, fixed the output of the signal generators to no greater than -30 dBm and input to the system of -41 dBm.

The noise figure and gain measurements were taken from the noise figure plots. These curves tended to be noisy due to the isolators not being able to completely eliminate all the reflections to the laser that were coming back from the phase matching devices. Therefore averaging was used in order to provide for smoother curves.

The equation for the maximum dynamic range is:

$$(17) \quad \text{Dynamic Range}_{max}(dB) = [12dBm - G_{amp} - G_{Sys}] - [F + 10 \text{ Log } kTB]$$

where the term in the first bracket is the maximum allowable power into the system. The equation for the spurious free dynamic range is the same as used for the amplifier calculations. The equations for the link fundamental and IM product lines are:

Trans/Receiver/ Amp SN	
T-23/R-92/130263	$P_{out\ (Fundamental\ Curve)}(dBm) = 0.96 * P_{in}(dBm) - 12.30$
	$P_{out\ (Third\ Order\ Curve)}(dBm) = 2.34 * P_{in}(dBm) + 36.21$
T-66/R-28/130262	$P_{out\ (Fundamental\ Curve)}(dBm) = 1.04 * P_{in}(dBm) - 2.68$
	$P_{out\ (Third\ Order\ Curve)}(dBm) = 4.20 * P_{in}(dBm) + 128.4$
T-64/R-30/130260	$P_{out\ (Fundamental\ Curve)}(dBm) = 0.97 * P_{in}(dBm) - 8.15$
	$P_{out\ (Third\ Order\ Curve)}(dBm) = 2.43 * P_{in}(dBm) + 34.85$
T-67/R-32/130261	$P_{out\ (Fundamental\ Curve)}(dBm) = 1.02 * P_{in}(dBm) - 7.77$
	$P_{out\ (Third\ Order\ Curve)}(dBm) = 3.00 * P_{in}(dBm) + 56.00$

Link, Amp, and Isolator	Third Order Intercept Point (dBm)	Maximum Dynamic Range (dB)		Spurious Free Dynamic Range (dB)		Noise Figure (dB)	Gain (dB)
		10 MHz	50 MHz	10 MHz	50 MHz		
T-23;R-92 130263	-35	40	33	26	21	15	-11
T-66;R-28 130262	-41	49	42	33	28	14	-4
T-64;R-30 130260	-30	35	28	27	23	22	-7
T-67;R-32 130261	-32	38	31	31	27	16	-10
Average	-35	41	34	29	25	17	-8

Table 3: Tabulated results for the time matched systems.

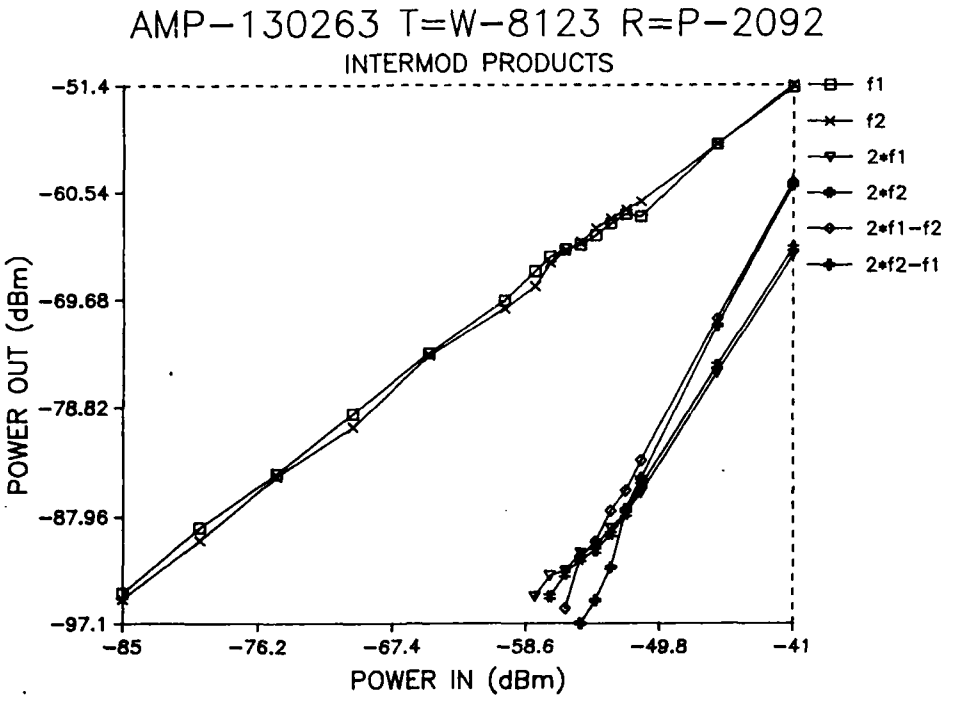

Figure 19: Intermod and Dynamic Range Characteristic Curves

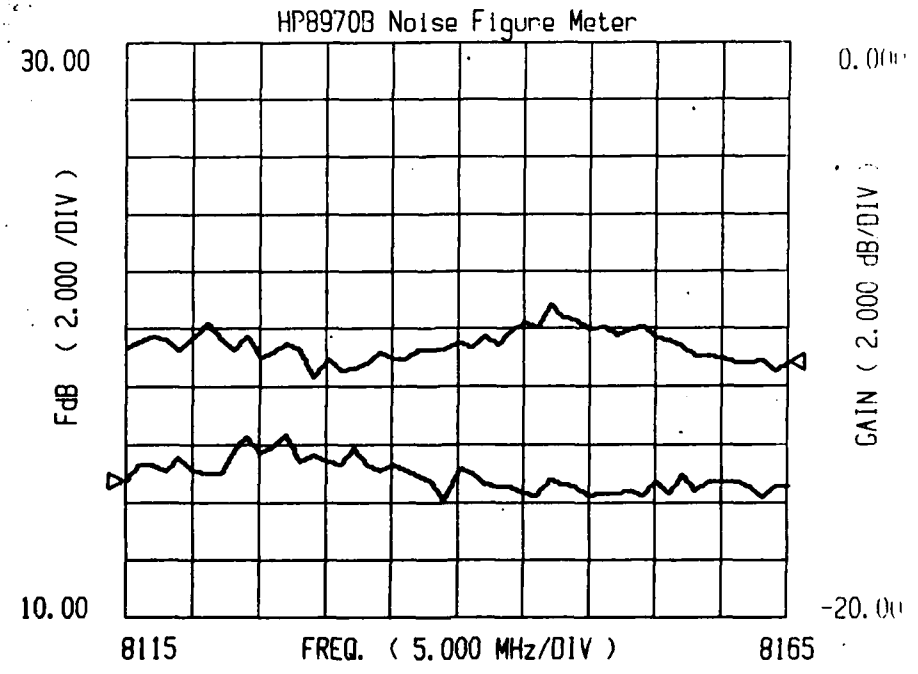

Figure 20: Noise Figure and Gain Plot

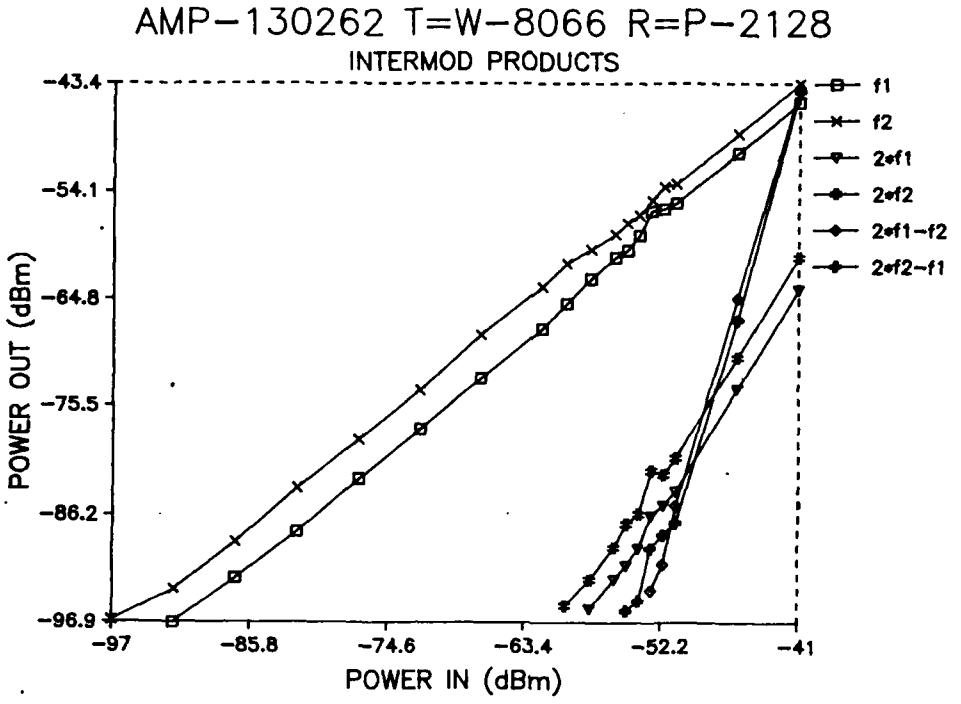

Figure 21: Intermod and Dynamic Range Characteristic Curves

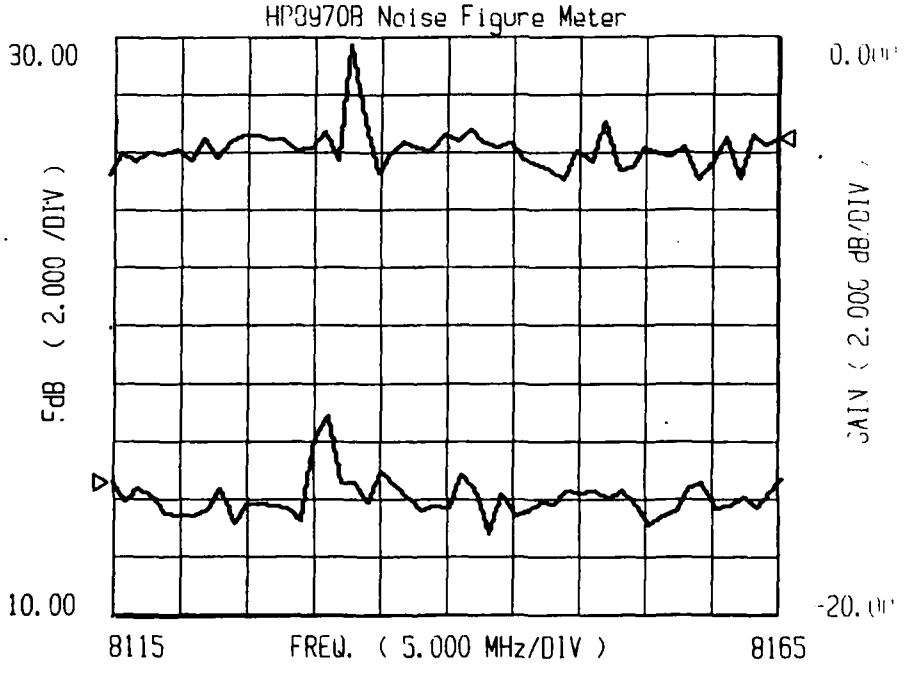

Figure 22: Noise Figure and Gain Plot

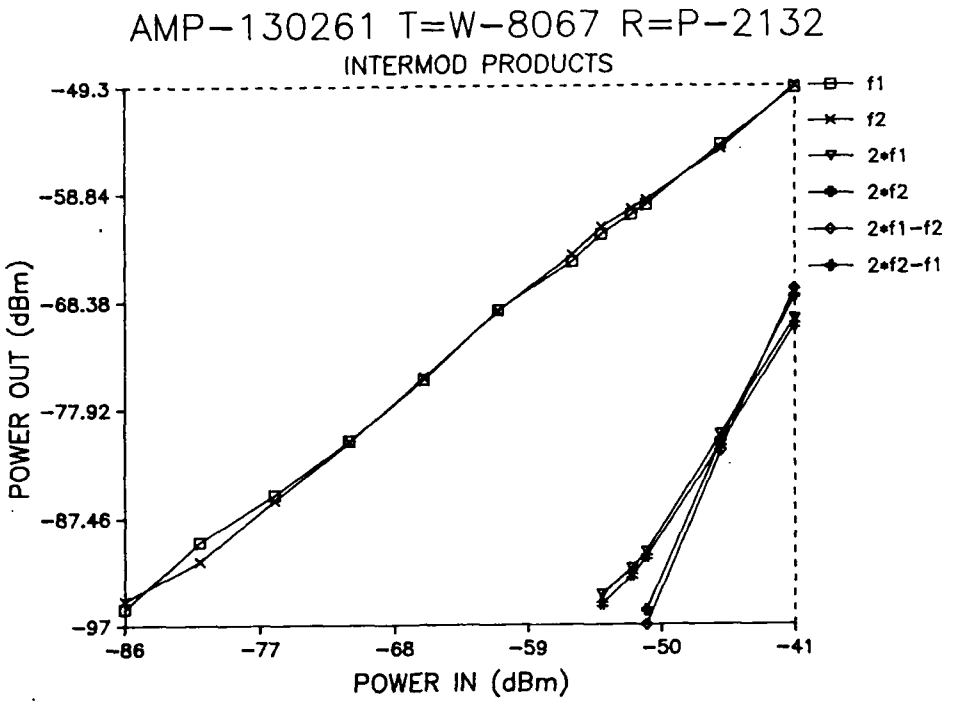

Figure 23: Intermod and Dynamic Range Characteristic Curves

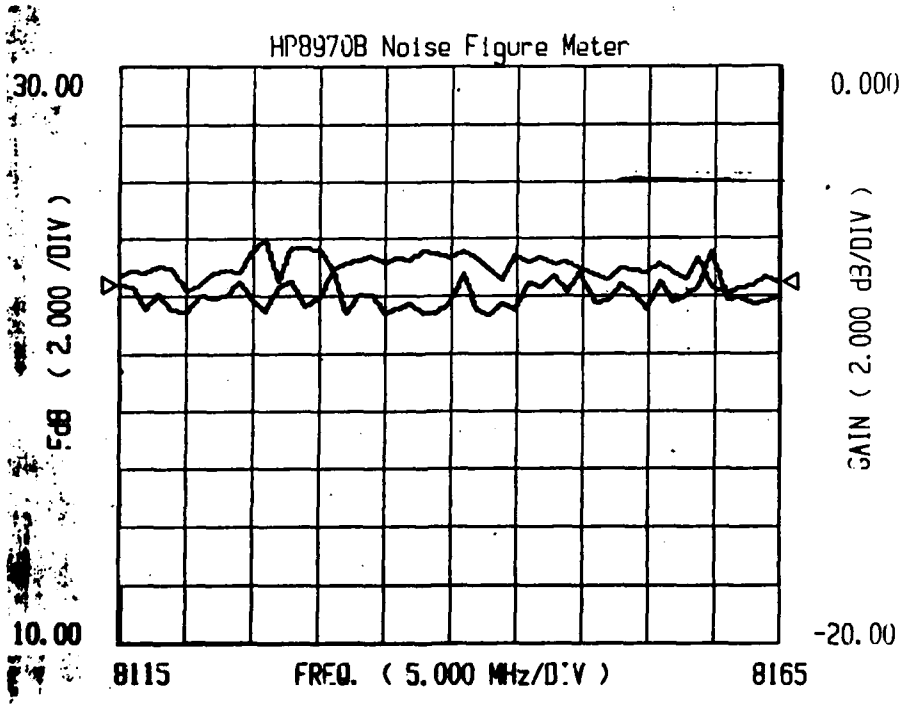

Figure 24: Noise Figure and Gain Plot

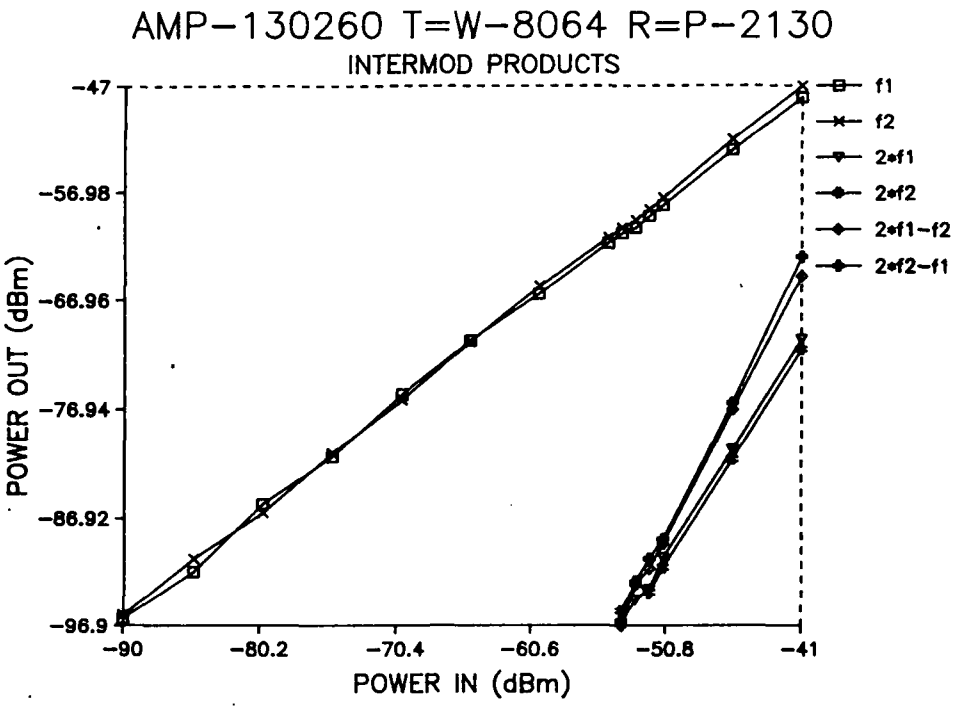

Figure 25: Intermod and Dynamic Range Characteristic Curves

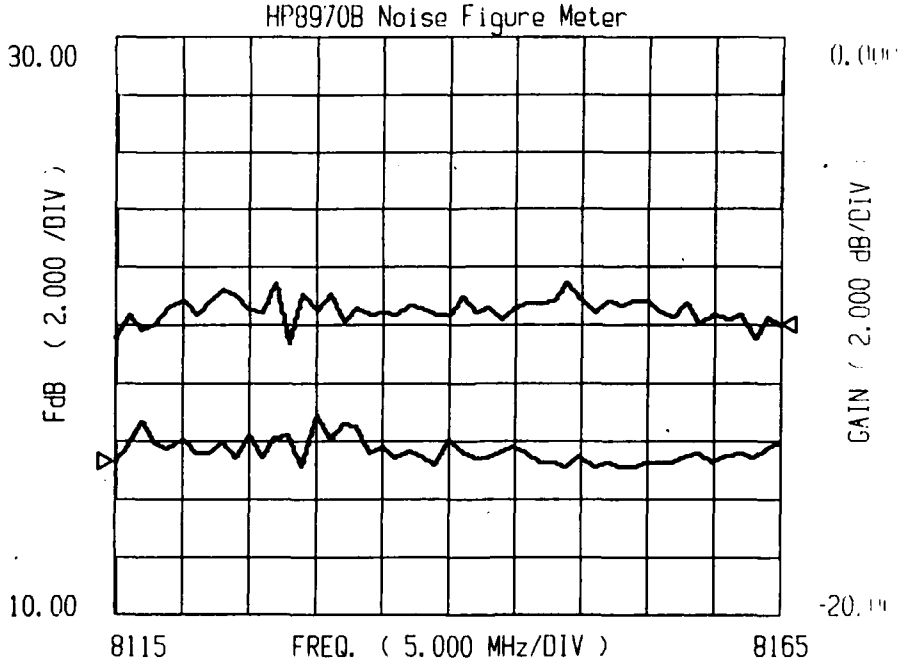

Figure 26: Noise Figure and Gain Plot

5. Conclusion and Recommendations

It is desirable to have the optical links appear transparent to your system, much as you would expect cabling to be relatively transparent. This is an unrealistic expectation since unlike cabling, optical links consist of active as well as passive devices.

The active devices such as the amplifier, detectors, and lasers add unwanted noise as well as signal nonlinearities. The noise limits our maximum dynamic range, while with the additional nonlinearities our spurious free dynamic range is limited even more. The greatest limitation to our dynamic range was due to the optical links (laser and detector pair) themselves. This is mostly due to the inefficiencies of the laser transmitter. A typical system might require maximum dynamic range and spurious free dynamic ranges in excess of 70 and 50 dB in the MHz bandwidth range, respectively. The systems we characterized fell short of this mark on the order of 20 to 30 dB but delivered usable dynamic range values for use in the DCCD anechoic chamber.

A significant drop between the combined gain of the amplifiers and links, and completed systems is due to the numerous passive devices (optical isolators, biconic connectors, and phase matching device) inserted in the fiber. Greater electronic amplification would be needed in order to realize no attenuation of the signal for our optical link systems. Perhaps a better approach would be to perform the phase matching in the coax. This would eliminate the losses associated with the phase matching device and therefore the need for the optical isolators (and thereby also eliminate their loss). Considering their high insertion loss, it is probably more economical to utilize these devices in long haul systems where the low attenuation in fiber can be more fully appreciated.

For a typical system we would probably want to limit the noise figure to no greater then the noise figure of our receiver, which would probably be on the order of 10 dB. Our systems exceeded that amount on average by 7 dB. Since the availability of high speed commercial links is so limited, this result will have to be tolerated for the present. However this indicates that noise is an important area for future work. One possible method for lowering noise would be the use of continuous lasers with external modulators[6]. Additional effort in the area of efficient power transfer from the RF source to the laser diode is also required.

REFERENCES

1. Morris Engelson, "Measuring IMD By Properly Using The Spectrum Analyzer", Microwaves & RF, February 1988, pp. 85-90.

2. Morris Engelson, "Define Dynamic Range For Better Spectrum Analysis", Tektronix.

3. "Spectrum Analysis"; Hewlett Packard, Application Note 150, Nov 89.

4. "RF and Microwave Signal Analysis Measurement Seminar", Hewlett Packard, Feb 88.

5. "Noise Figure Measurements; Principles and Applications", Hewlett Packard, April 1988.

6. G.E. Betts, L.M. Johnson, C.H. Cox III, and S.D. Lowney; "High-Performance Optical Analog Link Using External Modulator"; IEEE Photonics Technology Letters; vol. I, no. 11, pp. 404-406, Nov 89.

MISSION
of
Rome Air Development Center

RADC plans and executes research, development, test and selected acquisition programs in support of Command, Control, Communications and Intelligence (C^3I) activities. Technical and engineering support within areas of competence is provided to ESD Program Offices (POs) and other ESD elements to perform effective acquisition of C^3I systems. The areas of technical competence include communications, command and control, battle management information processing, surveillance sensors, intelligence data collection and handling, solid state sciences, electromagnetics, and propagation, and electronic reliability/maintainability and compatibility.